Title
Microstructure, crystallization and shape memory behavior of titania and yttria co-doped zirconia

Journal
Journal of the European Ceramic Society, 36(5)

ISSN
0955-2219

Authors
Zeng, Xiao Mei
Du, Zehui
Schuh, Christopher A
et al.

Publication Date
2016-04-01

DOI
10.1016/j.jeurceramsoc.2015.11.042

Peer reviewed

journal
of the American Ceramic Society

Microstructure, Crystallization and Shape Memory Behavior of Titania and Yttria Co-Doped Zirconia

Journal:	*Journal of the American Ceramic Society*
Manuscript ID:	JACERS-36841
Manuscript Type:	Article
Date Submitted by the Author:	13-May-2015
Complete List of Authors:	Zeng, Xiao Mei; Nanyang Technological University, Temasek Laboratories; Nanyang Technological University, School of Materials Science and Engineering Du, Zehui; Nanyang Technological University, Temasek Laboratories Schuh, Christopher; Massachusetts Institute of Technology, Department of Materials Science and Engineering Tamura, Nobumichi; Lawrence Berkeley National Lab, Gan, Chee Lip; Nanyang Technological University, Temasek Laboratories; Nanyang Technological University, School of Materials Science and Engineering
Keywords:	titanium dioxide, zirconia: yttria stabilized, crystals/crystallization, segregation

Microstructure, Crystallization and Shape Memory Behaviour of Titania and Yttria Co-Doped Zirconia

*Xiao Mei Zeng[1,2], Zehui Du[1], Christopher A Schuh[3], Nobumichi Tamura[4], Chee Lip Gan[1,2]**

Xiao Mei Zeng, Zehui Du, Prof. Chee Lip Gan*

[1]. Temasek Laboratories, Nanyang Technological University, Singapore, 637553

* Corresponding author: Chee Lip Gan, CLGan@ntu.edu.sg,

Xiao Mei Zeng, Prof.Chee Lip Gan

[2]. School of Materials Science and Engineering, Nanyang Technological University, Singapore, 639798

Prof.Christopher A Schuh

[3]. Department of Materials Science and Engineering, Massachusetts Institute of Technology, Cambridge, MA, USA, 02139

Dr. Nobumichi Tamura

[4]. Advanced Light Source (ALS), Lawrence Berkeley National Laboratory (LBNL), Berkeley, California, USA, 94720

Abstract

Small volume zirconia ceramic samples with few or no grain boundaries have been demonstrated recently to exhibit the shape memory effect with large strains. To explore the shape memory properties of yttria stabilized zirconia (YSZ), it is desirable to develop large, microscale grains, instead of the normally submicron grains that result from typical processing of YSZ. In this work, titania has been doped into YSZ ceramics and the effects of titania doping on the grain growth, crystallization and microscale elemental distribution of the ceramics have been systematically studied. With 5 mol% titania doping, the grain size can be increased up to ~3 μm through a conventional sintering cycle, while retaining a large quantity of the desired tetragonal

* Corresponding author: Chee Lip Gan, CLGan@ntu.edu.sg.

phase of zirconia. Such ceramics partition into two phases with different compositions, i.e. tetragonal phase with ~2 mol% yttria and cubic phase with ~5 mol% yttria. Micro-pillars machined from the 2 mol% yttria grains, and thus in the tetragonal phase, exhibited significantly enhanced shape memory effect in comparison to those without titania.

Keywords: titania doping, YSZ, microstructure, crystallization, elemental analysis, shape memory effect

Introduction

Tetragonal zirconia has been intensively investigated due to its martensitic transformation between the metastable tetragonal phase and the thermally stable monoclinic phase at low temperatures.[1] This diffusionless, displacive transformation can be induced by an external stress or a change in temperature, and involves a significant shear strain and volume change.[2] The resulting dramatic strain evolution and redistribution that occurs upon transformation is the source of transformation toughening[3] in bulk zirconia ceramics, as well as potential shape memory and superelastic properties [4]. A few oxides have been found effective in stabilizing the tetragonal phase of zirconia at room temperature, such as CeO_2[5], MgO[6] and Y_2O_3[7]. Among these, Y_2O_3 is considered the most effective stabilizer as less than 4 mol% is sufficient to fully stabilize the tetragonal phase.[8] Numerous studies have been made on the phase transformation in yttria stabilized tetragonal zirconia polycrystals (Y-TZP).[9, 10] However, there is a general lack of observations of shape memory properties in Y-TZP, although they have been described in the related ceria doped zirconia systems for about three decades.[11, 12]

Due to the large ionic radius of yttrium, its diffusion in zirconia is slow, and Y-TZP therefore generally enjoys a low grain growth rate. Typical powder processed Y-TZP generally has submicron grains as well as an inhomogeneous Y_2O_3 distribution.[13] Since small grains tend to

suppress the martensitic transformation, when such polycrystals are subjected to applied stress, cracks are generally initiated before achieving observable shape deformation via the transformation. On the other hand, in our recent work[14], we showed that for small-volume samples with a length scale reduced to a few micrometers, zirconia ceramics will have an oligocrystalline structure and can exhibit significantly enhanced shape memory properties without cracking. In that work, we used Ce-containing zirconia with a grain size of about 2 μm. While it would be interesting to explore small samples of conventional Y-TZP for shape memory properties, their small grain size would require commensurately smaller test samples (submicron). Alternatively, methods to increase the Y-TZP grain size from submicron to micron scale without suppressing the martensitic transformation behavior are also of interest.

The grain growth of zirconia is found to be controlled by the dopant material and sintering temperature.[15] For example, large crystals of Y-TZP can be obtained by sintering it at very high temperatures around 2500°C (skull sintering), [16] while some additives such as MgO, CeO_2, Nb_2O_5, and TiO_2 are reported to favor larger grains in zirconia during sintering at lower temperatures.[17-19] In the present work, we favor the latter approach of using dopants to increase grain size, and such additives should be selected based on at least the following criteria: (1) the additive oxide should be able to promote grain growth, (2) the martensitic transformation behavior should be retained, (3) the additive oxide should not lead to the formation of any undesired phases (i.e. cubic, monoclinic), and (4) the dopant should be stable through high temperature sintering without considerable evaporation or forming a porous structure.

Based on our preliminary experimental results (not reported here) as well as supporting information from literature[20], titania (TiO_2) was found to satisfy the above criteria. The experiments in this work were therefore designed with the goal of fabricating Y_2O_3-TiO_2-ZrO_2

ternary ceramics with microscale grains suitable for micromechanical testing of shape memory properties.

Experimental

Literature work has revealed that about 2 to 4 mol% of Y_2O_3 is effective in stabilizing the majority of zirconia in the tetragonal phase[1]. The slightly larger Y^{3+} cations (0.1019 nm) substitute for the host Zr^{4+} cations (0.084 nm) inside the crystal[19], introducing oxygen vacancies to balance the charge between cation and anion[21]. These oxygen vacancies are believed to be stabilizing the tetragonal phase. Less than 10 mol% of TiO_2 was introduced in this work, as excess TiO_2 can react with zirconia to form $ZrTiO_4$ at temperatures above 1400°C[22].

The starting materials were commercial 3 mol% yttria doped zirconia with a particle size of 40 nm (TZ-3Y-E grade, Tosoh, Japan), TiO_2 (≥99%) and Y_2O_3 (≥99.99%) (Sigma-Aldrich, USA) powders. The ceramic powders were mixed according to the formula xY_2O_3-$yTiO_2$-(100-x-y)ZrO_2 with x = 0-6 and y = 0-10, by adding pure oxide into the TZ-3Y powders. The mixed powders were ball milled with zirconia milling balls for 24 hours to obtain a homogeneous powder mixture. The powders were then combined with 0.35 wt% polyvinyl alcohol (PVA) with Mw = 72k as binder and pressed into pellets using a hydraulic press at 100 MPa. The green pellets were further pressed at 35 MPa with a cold isostatic press (CIP). To prevent the production of pores as a result of PVA decomposition during sintering, the pellets were pre-sintered to pyrolyze the PVA, followed by a second CIP step to further densify the ceramics. The pellets were then sintered at 1500 or 1700°C for 6 hours at a heating rate of 5°C/min. Finally, the sintered pellets were polished with diamond slurry and hot etched at 1450 or 1650°C for 30 min.

Detailed microstructural characterization of the hot-etched ceramic surface was performed with field emission scanning electron microscopy (FESEM, JOEL 7600F). The grain size was

analyzed with image analysis software (ImageJ, National Institutes of Health, West Bethesda, MD).[23] The phase composition of the ceramics was studied by x-ray diffraction (XRD, D8, Bruker) with Cu Kα radiation. The spatial elemental distribution across different grains was mapped with electron probe micro-analysis (EPMA, JXA-8500F, JEOL). The crystal structure of some individual grains was studied by synchrotron radiation scanning X-ray micro-diffraction (μXRD) technique using a white beam[24] on beamline 12.3.2 at the Advanced Light Source, Berkeley, CA. The μXRD patterns were collected using a DECTRIS Pilatus hybrid pixel array detector and analyzed using the XMAS (μXRD analysis software) software package.

Based on the EPMA maps, some grains were chosen and machined into pillars with dimensions of ~1 μm × 3.5 μm (diameter × height) using Focused Ion Beam milling system (FIB, FEI Nova 600i Nanolab). To study the shape memory effect, the pillars were compressed with a nanoindenter (Hysitron, TI950) equipped with a 20 μm spherical-conical diamond tip. The loading and unloading rate of the compression was 50 μN/sec. After compression, the pillars were heat-treated at 500^{o}C to explore shape recovery.

Results & discussion

To illustrate the effect of TiO_2 on the grain growth of zirconia, its concentration was varied while Y_2O_3 doping was kept constant at 3 mol%. The average grain size with respect to the TiO_2 concentration is shown in Figure 1(a), as well as the respective microstructure of each composition. Clear grain boundaries can be observed in the SEM images and no visible pores are found. The grain size was significantly increased from 0.5 μm to 4 μm with 5 mol% TiO_2 added. This observation is in agreement with literature that TiO_2 could promote grain growth[25, 26], as it can enhance the average diffusion rate during sintering. Higher doping of 10 mol% TiO_2 did not

significantly change the grain size, most probability due to the saturation of TiO_2. Literature work found that the solubility of TiO_2 in Y-TZP is lower than 13 mol% at 1700°C.[27, 28]

Figure 1(b) provides further detail on the effects of doping for the Y_2O_3-ZrO_2 binary and $x$$Y_2O_3-5TiO_2$-$ZrO_2$ ternary systems. Varying the Y_2O_3 concentration at a sintering temperature of 1500°C had no clear effect upon the grain size for the binary Y_2O_3-ZrO_2 system, which remained fairly constant in the range between 0.4 - 0.5 μm. A higher sintering temperature at 1700°C only slightly increased the grain size to an average of 0.55 μm in the binary system. On the other hand, by adding 5 mol% TiO_2, the grain size of $x$$Y_2O_3-5TiO_2$-$ZrO_2$ for 2 to 4 mol% of Y_2O_3 significantly increased to an average of 3.1 μm. Compared to prior studies of 10 mol% TiO_2 at 1400°C,[26] we found that 5 mol% of TiO_2 works similarly in promoting grain growth at a higher temperature of 1700°C, but did not lead to the formation of the undesired $ZrTiO_4$ compound.

Effect of TiO_2 and Y_2O_3 co-doping on phase content

Chemical composition is a key factor for martensitic transformation of zirconia, regardless of the grain size. The phase content of both Y_2O_3-ZrO_2 binary and Y_2O_3-TiO_2-ZrO_2 ternary systems has been studied by XRD, as shown in Figure 2(a) and 2(b). In the effort to resolve the overlapped XRD profiles for monoclinic, tetragonal and cubic phase of the ceramics, a full scan with 2θ = 25-90° and a fine scan with 2θ = 70-76° were conducted according to Srinivasan *et al.* [29]. Analysis of the peak positions from the XRD spectrum confirmed that there were no non-zirconia phases such as rutile TiO_2 or $ZrTiO_4$ present in the ceramics[26].

The monoclinic, tetragonal and cubic phases in both Y_2O_3-ZrO_2 and $x$$Y_2O_3-5TiO_2$-$ZrO_2$ systems can be discerned from the characteristic peaks for the corresponding phase[30]. As shown in Figure 2(a), peak $(111)_m$ and $(11\bar{1})_m$ signify the presence of monoclinic phase, whereas peak

$(111)_{t/c}$ denotes the presence of either the tetragonal or cubic phase. The tetragonal phase can be further differentiated from the cubic phase by resolving the $(400)_t$ and $(004)_t$ peaks of the tetragonal phase from the peak $(400)_c$ of the cubic phase, as shown in Figure 2(a). From the relative intensities of the characteristic peaks in Figure 2, it seems clear that the ceramic is dominated by monoclinic phase for $Y_2O_3 \leq 2$mol%, whereas majority of tetragonal phase can be found for Y_2O_3 between 2.5 to 4 mol%. Further increase of the Y_2O_3 level leads to more cubic phase, which is not the desired phase for martensitic transformation, and so of little interest to the present work.

The weight fraction of the monoclinic phase ($\boldsymbol{X_m}$) with respect to the tetragonal/cubic phase ($\boldsymbol{X_{t/c}}$) can be quantified based on the relative intensities of the peaks according to the following equation:[31]

$$\boldsymbol{X_m} = \frac{\boldsymbol{I(11\bar{1})_m + I(111)_m}}{\boldsymbol{I(11\bar{1})_m + I(111)_m + I(111)_{t/c}}} = \mathbf{1} - \boldsymbol{X_{t/c}} \quad \text{---------- (1)}$$

where I $(111)_m$, I$(11\bar{1})_m$ and I$(111)_{t/c}$ are the integrated intensity from the monoclinic (111), $(11\bar{1})$ peaks and tetragonal/cubic (111) peak, respectively. Further quantitative differentiation of the tetragonal and cubic phase fractions is not accurate, as the respective peaks are not fully resolved and the intensities are relatively weak compared to the background; we will turn to another method of resolving these two phases in a later section. Nonetheless, the data in Figure 3 show that the weight fraction of monoclinic phase decreases with the introduction of Y_2O_3, which fully stabilizes the tetragonal/cubic phase to room temperature at 4mol% of Y_2O_3.

TiO_2 doping also contributes to the stabilization of the tetragonal/cubic phase and suppresses the formation of monoclinic phase. By adding 5 mol% TiO_2 into the Y_2O_3-ZrO_2 ceramics, the fraction of tetragonal/cubic phase significantly increases for $Y_2O_3 \leq 3.5$mol%. According to

Figure 3, there is no monoclinic phase in $x$$Y_2O_3-5TiO_2$-$ZrO_2$ for $Y_2O_3 \geq 2.5$mol%, and the ceramic is fully composed of tetragonal and cubic phases.

The effect of TiO_2 doping on the lattice constants of 3Y_2O_3-$y$$TiO_2$-$ZrO_2$ ceramics is shown in Figure 4. For TiO_2 doping less than 10 mol%, the tetragonal lattice constant a_t decreases, while c_t increases with TiO_2 concentration. This can be attributed to the smaller ionic diameter of titanium (0.074 nm)[19] as compared to zirconium. For 3Y_2O_3-ZrO_2 binary ceramics, the lattice constants are $a_t = 5.0983$ Å, $c_t = 5.1814$ Å. These lattice constants are in good agreement with the tetragonal 2Y_2O_3-ZrO_2 ceramics reported in the literatures (a = 5.1003 Å, c = 5.1866 Å)[32, 33]. With 5 mol% TiO_2 doping, the lattice constants are changed to $a_t = 5.0930$Å, $c_t = 5.1840$Å, and thus increase the tetragonality (c_t/a_t) of zirconia. This result follows expectations of Vegard's law of solid solution[27].

Chemical heterogeneity

Previous work on the Y_2O_3-ZrO_2 system[34] using processing methods similar to ours has revealed signatures of inhomogeneous distribution of Y_2O_3 in the zirconia matrix, especially after long exposures to high sintering temperatures. The characteristic XRD peaks in Figure 2 also suggested a mixture of tetragonal and cubic phases for $Y_2O_3 \geq 2.5$mol%, and how the two phases are distributed at the grain-scale needs further characterization. More importantly, whether co-doping with TiO_2 can affect the spatial chemical and phase distribution in the ternary Y_2O_3-TiO_2-ZrO_2 system remains a question.

Chemical mapping was conducted by EPMA on the surface of both 3Y_2O_3-ZrO_2 and 3Y_2O_3-5TiO_2-ZrO_2 ceramics, across a typical area of 200 μm × 200 μm, as shown in Figure 5. We identify two distinct elemental compositions that predominate the observations in general, which we term "high yttrium regions" (HYR) (in green) and "low yttrium regions" (LYR) (in blue).

This elemental segregation is found to take on a finer length scale in the binary $3Y_2O_3$-ZrO_2 ceramic, with typical domain areas of ~ 1 μm^2 for both HYR and LYR, as compared to ~ 4 μm^2 in the ternary $3Y_2O_3$-$5TiO_2$-ZrO_2. This size difference is in good agreement with the grain sizes of the two systems.

Finer elemental maps, together with corresponding SEM images, are illustrated in Figure 6. By comparing the grain structure seen in the SEM image with the elemental maps, one can see that the yttrium segregation into LYR and HYR domains occurs in a grain-wise fashion. There is no clear suggestion of localization at grain boundaries as suggested by Schelling *et al.*[13] Yttrium has a low solubility in the tetragonal zirconia crystal structure[13], so the excess yttrium tends to accumulate in the cubic phase. The titanium distribution is rather homogeneous as compared to yttrium, which is expected as titanium solubility in tetragonal zirconia is higher than 5 mol%.

EPMA mapping was carried out on another two ceramics with different Y_2O_3 concentrations, i.e. $2.5Y_2O_3$ -$5TiO_2$-ZrO_2 and $4Y_2O_3$-$5TiO_2$-ZrO_2. A quantitative composition analysis on the respective grains within LYR and HYR are shown in Figure 7(a) for the three ceramics with different global doping concentrations. Just as seen above, these materials all exhibit chemical partitioning into HYR and LYR, in a manner that is relatively consistent across the samples of different global composition. The HYR generally have about 5 mol% Y_2O_3 and are easily distinguished from the LYR at about 2 mol% Y_2O_3, as illustrated in Figure 7(a). According to Matsui *et al.*[13], the solubility of Y_2O_3 in tetragonal zirconia is less than 3 mol% when sintered at 1400°C and it should be lower for sintering temperature of 1700°C. Therefore, all of the data align with the interpretation that the LYR and HYR correspond to tetragonal and cubic phases, respectively. The volume fractions of the two phases (as assessed stereologically) change linearly with the global composition, as shown in Figure 7(b). The volume fraction of cubic

phase increases significantly from ~16% to ~38%, while the tetragonal phase decreases from ~84% to ~62%, as the global Y_2O_3 doping level increases from 2.5 to 4 mol%.

To confirm that the grains in the LYR regions were tetragonal, individual grains were taken out from the $3Y_2O_3$-$5TiO_2$-ZrO_2 ceramics using an Omni-Probe™ attached to an FEI Nova 600i Nanolab FIB/SEM system, and then analyzed by synchrotron radiation scanning X-ray micro-diffraction (μXRD). Figure **8**(a) shows one example SEM image of a grain from the LYR region, with Figure **8**(b) the corresponding Laue diffraction orientation map. The color indicates the misorientation across the sample, and the difference between the red and dark purple regions is only about 0.1°, confirming that the sample is a single crystal. The diffraction pattern in Figure **8**(c) has been indexed to tetragonal zirconia. Similar μXRD analysis on many grains from similar LYR areas identified the tetragonal phase exclusively. It is therefore confirmed that the $3Y_2O_3$-$5TiO_2$-ZrO_2 ceramics consist of tetragonal grains with ~2 mol% Y_2O_3 and cubic grains of HYR of ~ 5 mol% Y_2O_3. Since the xY_2O_3-$5TiO_2$-ZrO_2 ternary system comprises a large amount of tetragonal phase over a larger range of Y_2O_3 concentrations, it is regarded as a promising candidate as a shape memory ceramic.

Shape memory effect

The introduction of TiO_2 not only promotes grain growth in yttria-zicronia ceramics, which enables the fabrication of single crystal micropillars, it also significantly increases the prevalence of the tetragonal phase that is amenable to martensitic transformation.

The shape memory effect in $3Y_2O_3$-$5TiO_2$-ZrO_2 ceramics was studied by machining selected grains from the LYR area into micro pillars, followed by microcompression and heat treatment. The results are shown in Figure 9, together with one pillar from a binary $3Y_2O_3$-ZrO_2 ceramic for comparison. The $3Y_2O_3$-ZrO_2 pillar exhibits brittle behavior with fracture occurring immediately

after elastic deformation. In contrast, the $3Y_2O_3$-$5TiO_2$-ZrO_2 pillar shows large apparent malleability, sustaining ~ 800 nm of displacement without failure. The rapid burst of displacement without apparent hardening is a signature of the martensitic transformation. After unloading, there is a substantial residual displacement, consistent with direct observation of unrecovered deformation (bending) in the respective SEM image. Treating the pillar as a simple point-loaded cantilever beam, the compressive strain on the inner side of the pillar is estimated to be ~7%.

To examine whether the pillar exhibits the shape memory effect, it was heated to 500^{O}C for 30 min, following which the SEM shows that the pillar has almost fully recovered its shape. The contrast between this behavior and that of the binary ceramic is significant; although both are tetragonal and capable of stress-induced martensitic transformation; only the ternary ceramics exhibit shape memory properties. We expect that this difference can most likely be attributed to the larger grain size of the ternary alloy, which makes it possible to machine the pillars that contain no (or very few) grain boundaries, yielding an oligocrystal or a single crystal. In our previous work, we showed that in zirconia ceramics polycrystals are brittle, whereas oligocrystals are not[35], and this would appear to be the key issue in the present samples.

Conclusion

In conclusion, the effects of TiO_2 doping on the microstructure, crystallization behavior and spatial elemental distribution of Y_2O_3-TiO_2-ZrO_2 ceramics have been systematically studied and a corresponding improvement in shape memory properties in micron-scale pillars of the TiO_2 doped ceramics has been demonstrated. The introduction of TiO_2 significantly promotes grain growth, and 5 mol% of TiO_2 is enough to achieve microscale tetragonal grains and enable single crystal or oligocrystal pillars for micro-mechanical testing. Doping with TiO_2 is also very

effective at stabilizing the tetragonal phase and suppressing the formation of monoclinic phase, which is further beneficial for shape memory properties; again the fraction of tetragonal phase is maintained up to ~84 vol% with 3 mol% of Y_2O_3. These ceramics comprise two types of grains, tetragonal grains with ~2 mol% Y_2O_3 and cubic grains with ~5 mol% Y_2O_3. Micropillars of $3Y_2O_3$-$5TiO_2$-ZrO_2 can be bent to large strains of order ~7% without cracking and almost fully recover their shape upon heating, hence demonstrating significantly enhanced shape memory properties.

Acknowledgement

We would like to thank Dr Liu Qing, Dr Jason Scott Herrin, Shahrouz Amini and Dr Ali Gilles Tchenguise Miserez at NTU for their assistance with experiments. We would like to acknowledge the project funding support under project agreements 9011102294 and 9011102296. The Advanced Light Source (ALS) is supported by the Director, Office of Science, Office of Basic Energy Sciences, of the U.S. Department of Energy under Contract No. DE-AC02-05CH11231 at the Lawrence Berkeley National Laboratory (LBNL).

References

1. J. Chevalier, L. Gremillard, A. V. Virkar and D. R. Clarke, "The Tetragonal-Monoclinic Transformation in Zirconia: Lessons Learned and Future Trends," *J Am Ceram Soc*, **92** [9] 1901-1920 (2009).
2. P. M. Kelly and C. J. Ball, "Crystallography of Stress-Induced Martensitic Transformations in Partially-Stabilized Zirconia," *J Am Ceram Soc*, **69** [3] 259-264 (1986).
3. A. G. Evans and A. H. Heuer, "Transformation Toughening in Ceramics - Martensitic Transformations in Crack-Tip Stress-Fields," *J Am Ceram Soc*, **63** [5-6] 241-248 (1980).
4. M. V. Swain, "Shape Memory Behavior in Partially-Stabilized Zirconia Ceramics," *Nature*, **322** [6076] 234-236 (1986).
5. K. H. Heussner and N. Claussen, "Strengthening of Ceria-Doped Tetragonal Zirconia Polycrystals by Reduction-Induced Phase-Transformation," *J Am Ceram Soc*, **72** [6] 1044-1046 (1989).
6. P. Duwez, F. Odell and F. H. Brown, "Stabilization of Zirconia with Calcia and Magnesia," *J Am Ceram Soc*, **35** [5] 107-113 (1952).

7. A. Suresh, M. J. Mayo, W. D. Porter and C. J. Rawn, "Crystallite and grain-size-dependent phase transformations in yttria-doped zirconia," *J Am Ceram Soc*, **86** [2] 360-362 (2003).
8. H. G. Scott, "Phase-Relationships in the Magnesia-Yttria-Zirconia System," *J Aust Ceram Soc*, **17** [1] 16-20 (1981).
9. R. H. J. Hannink, P. M. Kelly and B. C. Muddle, "Transformation toughening in zirconia-containing ceramics," *J Am Ceram Soc*, **83** [3] 461-487 (2000).
10. B. I. Ardlin, "Transformation-toughened zirconia for dental inlays, crowns and bridges: chemical stability and effect of low-temperature aging on flexural strength and surface structure," *Dent Mater*, **18** [8] 590-595 (2002).
11. P. E. Reyesmorel and I. W. Chen, "Transformation Plasticity of Ceo2-Stabilized Tetragonal Zirconia Polycrystals .1. Stress Assistance and Auto-Catalysis," *J Am Ceram Soc*, **71** [5] 343-353 (1988).
12. P. E. Reyesmorel, J. S. Cherng and I. W. Chen, "Transformation Plasticity of Ceo2-Stabilized Tetragonal Zirconia Polycrystals .2. Pseudoelasticity and Shape Memory Effect," *J Am Ceram Soc*, **71** [8] 648-657 (1988).
13. K. Matsui, H. Horikoshi, N. Ohmichi, M. Ohgai, H. Yoshida and Y. Ikuhara, "Cubic-formation and grain-growth mechanisms in tetragonal zirconia polycrystal," *J Am Ceram Soc*, **86** [8] 1401-1408 (2003).
14. A. Lai, Z. H. Du, C. L. Gan and C. A. Schuh, "Shape Memory and Superelastic Ceramics at Small Scales," *Science*, **341** [6153] 1505-1508 (2013).
15. R. M. German, "Coarsening in Sintering: Grain Shape Distribution, Grain Size Distribution, and Grain Growth Kinetics in Solid-Pore Systems," *Crit Rev Solid State*, **35** [4] 263-305 (2010).
16. D. Michel, L. Mazerolles and M. P. Y. Jorba, "Fracture of Metastable Tetragonal Zirconia Crystals," *J Mater Sci*, **18** [9] 2618-2628 (1983).
17. Y. Sakka, T. S. Suzuki, T. Matsumoto, K. Morita, K. Hiraga and Y. Moriyoshi, "Effect of titania and magnesia addition to 3 mol% yttria doped tetragonal zirconia on some diffusion related phenomena," *Solid State Ionics*, **172** [1-4] 499-503 (2004).
18. D. J. Kim, "Effect of Ta2o5, Nb2o5, and Hfo2 Alloying on the Transformability of Y2o3-Stabilized Tetragonal Zro2," *J Am Ceram Soc*, **73** [1] 115-120 (1990).
19. C. A. Bateman and M. R. Notis, "Coarsening Kinetics in Mg(Ca,Ti,Y)-Partially-Stabilized Zirconias," *J Am Ceram Soc*, **75** [6] 1566-1569 (1992).
20. M. M. R. Boutz, A. J. A. Winnubst and A. J. Burggraaf, "Yttria-Ceria Stabilized Tetragonal Zirconia Polycrystals - Sintering, Grain-Growth and Grain-Boundary Segregation," *J Eur Ceram Soc*, **13** [2] 89-102 (1994).
21. S. Fabris, A. T. Paxton and M. W. Finnis, "A stabilization mechanism of zirconia based on oxygen vacancies only," *Acta Mater*, **50** [20] 5171-5178 (2002).
22. C. Wagner, "Theorie Der Alterung Von Niederschlagen Durch Umlosen (Ostwald-Reifung)," *Z Elektrochem*, **65** [7-8] 581-591 (1961).
23. C. Igathinathane, L. O. Pordesimo and W. D. Batchelor, "Major orthogonal dimensions measurement of food grains by machine vision using ImageJ," *Food Res Int*, **42** [1] 76-84 (2009).
24. A. S. Budiman, N. Li, Q. Wei, J. K. Baldwin, J. Xiong, H. Luo, D. Trugman, Q. X. Jia, N. Tamura, M. Kunz, K. Chen, and A. Misra, "Growth and structural characterization of epitaxial Cu/Nb multilayers," *Thin Solid Films*, **519** [13] 4137-4143 (2011).
25. F. Capel, C. Moure, P. Duran, A. R. Gonzalez-Elipe and A. Caballero, "Structure-electrical properties relationships in TiO2-doped stabilized tetragonal zirconia ceramics," *Ceram Int*, **25** [7] 639-648 (1999).

26. X. G. Miao, D. Sun, P. W. Hoo, J. L. Liu, Y. F. Hu and Y. M. Chen, "Effect of titania addition on yttria-stabilised tetragonal zirconia ceramics sintered at high temperatures," *Ceram Int*, **30** [6] 1041-1047 (2004).
27. F. Capel, M. A. Banares, C. Moure and P. Duran, "The solid solubility limit of TiO2 in 3Y-TZP studied by Raman spectroscopy," *Mater Lett*, **38** [5] 331-335 (1999).
28. L. S. M. Traqueia, T. Pagnier and F. M. B. Marques, "Structural and electrical characterization of titania-doped YSZ," *J Eur Ceram Soc*, **17** [8] 1019-1026 (1997).
29. R. Srinivasan, R. J. Deangelis, G. Ice and B. H. Davis, "Identification of Tetragonal and Cubic Structures of Zirconia Using Synchrotron X-Radiation Source," *J Mater Res*, **6** [6] 1287-1292 (1991).
30. N. Ohmichi, K. Kamioka, K. Ueda, K. Matsui and M. Ohgai, "Phase transformation of zirconia ceramics by annealing in hot water," *J Ceram Soc Jpn*, **107** [2] 128-133 (1999).
31. R. C. Garvie, "Phase Analysis in Zirconia Systems," *J Am Ceram Soc*, **55** [6] 303-305 (1972).
32. M. Hayakawa, N. Kuntani and M. Oka, "Structural Study on the Tetragonal to Monoclinic Transformation in Arc-Melted Zro2-2mol-Percent-Y2o3 .1. Experimental-Observations," *Acta Metall Mater*, **37** [8] 2223-2228 (1989).
33. M. Hayakawa and M. Oka, "Structural Study on the Tetragonal to Monoclinic Transformation in Arc-Melted Zro2-2mol-Percent-Y2o3 .2. Quantitative-Analysis," *Acta Metall Mater*, **37** [8] 2229-2235 (1989).
34. K. Matsui, H. Yoshida and Y. Ikuhara, "Grain-boundary structure and microstructure development mechanism in 2-8 mol% yttria-stabilized zirconia polycrystals," *Acta Mater*, **56** [6] 1315-1325 (2008).
35. Z. H. Du, X. M. Zeng, Q. Liu, A. Lai, S. Amini, A. G. T. Miserez, C. A. Schuh, and C. L. Gan, "Size effects and shape memory properties in micro/nano ZrO2 ceramic pillars," *Scripta Materialia*, **101** 40-43 (2015).

Figure Capture List

Figure 1: Average grain size of (a) $3Y_2O_3$-$y$$TiO_2$-$ZrO_2$ with different amounts of added TiO_2 and sintered at 1700°C, and (b) Y_2O_3-ZrO_2 and $x$$Y_2O_3-5TiO_2$-$ZrO_2$ doped with various amount of Y_2O_3, sintered at 1500°C or 1700°C.

Figure 2: XRD spectrum of (a) binary Y_2O_3-ZrO_2 system, and (b) ternary $x$$Y_2O_3-5TiO_2$-$ZrO_2$ system.

Figure 3: Calculated weight fraction (wt%) of monoclinic phase and the complementary tetragonal/cubic phases (which are not separated in this analysis) in binary Y_2O_3-ZrO_2 and ternary $x$$Y_2O_3-5TiO_2$-$ZrO_2$ system.

Figure 4: Lattice constants and tetragonality of the tetragonal phase in $3Y_2O_3$-TiO_2-ZrO_2 as a function of TiO_2 concentration.

Figure 5: EMPA mapping of yttrium in (a) $3Y_2O_3$-ZrO_2 and (b) $3Y_2O_3$-$5TiO_2$-ZrO_2 ceramics.

Figure 6: EMPA mapping of $3Y_2O_3$-$5TiO_2$-ZrO_2 ceramics, with the SEM images and elemental distributions at the corresponding area. The concentration colour scale is the same as presented in Figure 5.

Figure 7: (a) Localized concentration of Y_2O_3 for high yttrium region (HYR) and low yttrium region (LYR). (b) The phase fraction of tetragonal phase (LYR) and cubic phase (HYR) in $x$$Y_2O_3$-$5TiO_2$-$ZrO_2$ system.

Figure 8: (a) SEM image of the grain cut from the LYR region of $3Y_2O_3$-$5TiO_2$-ZrO_2 ceramics, (b) the orientation map of the grain, (c) the corresponding Laue diffraction pattern.

Figure 9: Load-displacement curves of $3Y_2O_3$-ZrO_2 and $3Y_2O_3$-$5TiO_2$-ZrO_2 pillars, and the corresponding SEM images before and after micro-compression, and after heating at 500^oC.

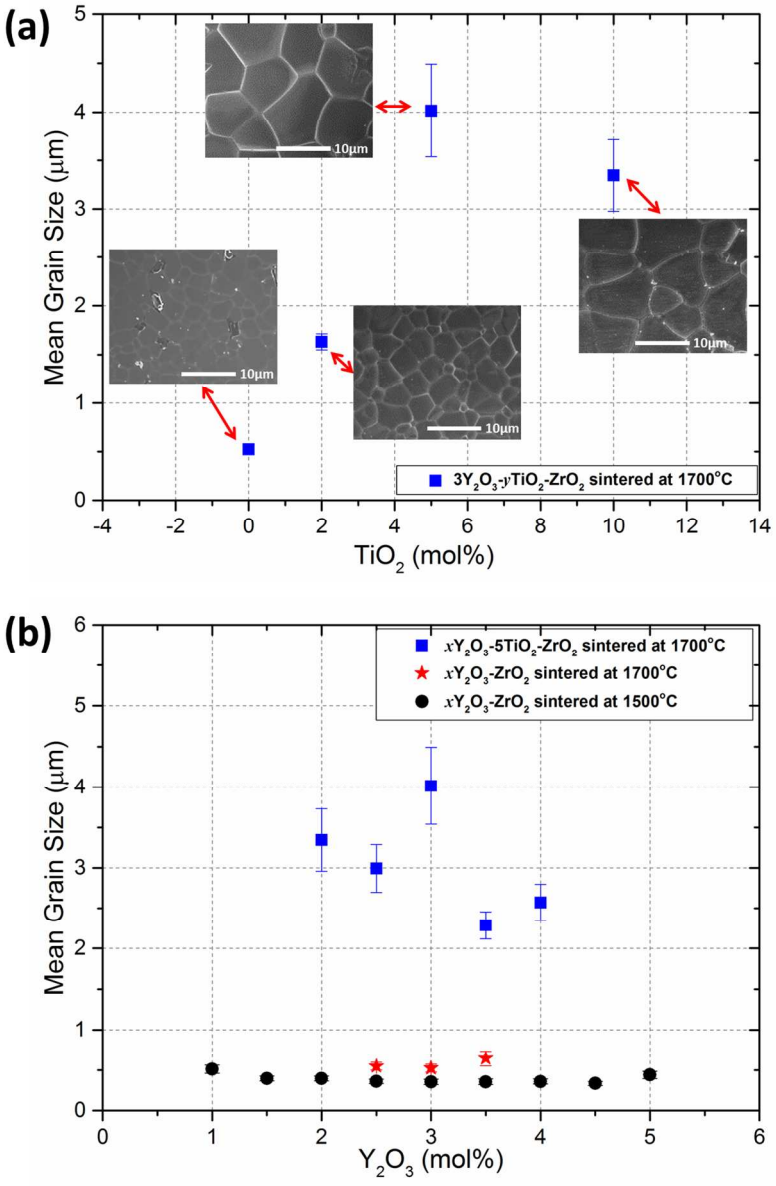

Figure 1: Average grain size of (a) 3Y2O3-yTiO2-ZrO2 with different amounts of added TiO2 and sintered at 1700oC, and (b) Y2O3-ZrO2 and xY2O3-5TiO2-ZrO2 doped with various amount of Y2O3, sintered at 1500oC or 1700oC.
238x357mm (150 x 150 DPI)

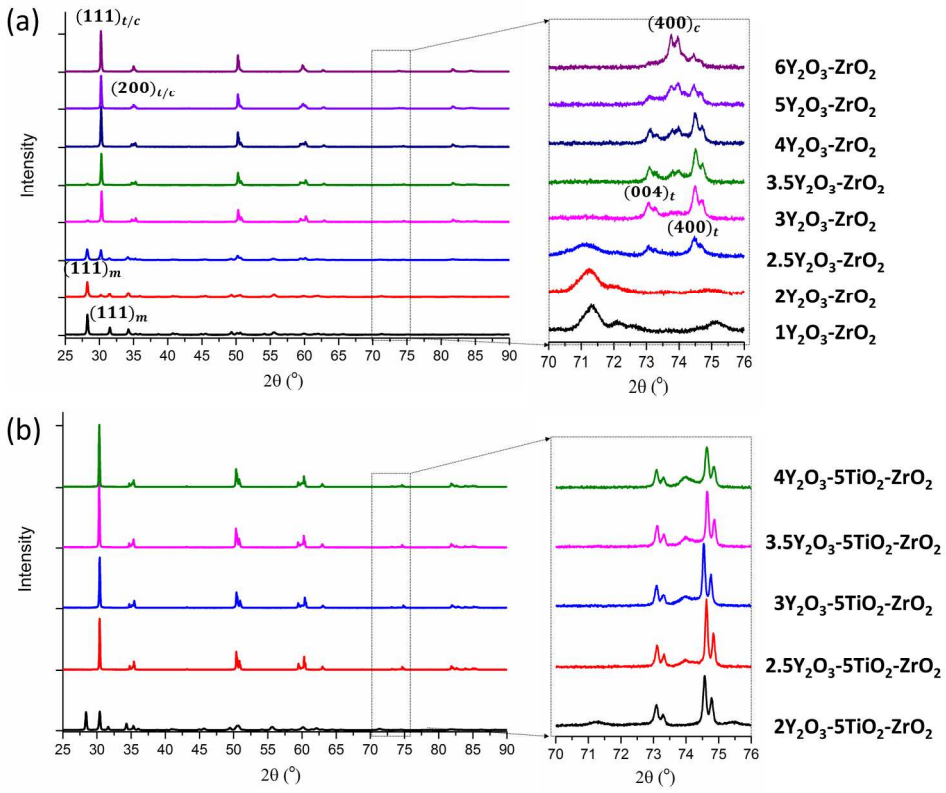

Figure 2: XRD spectrum of (a) binary Y2O3-ZrO2 system, and (b) ternary xY2O3-5TiO2-ZrO2 system.
440x354mm (150 x 150 DPI)

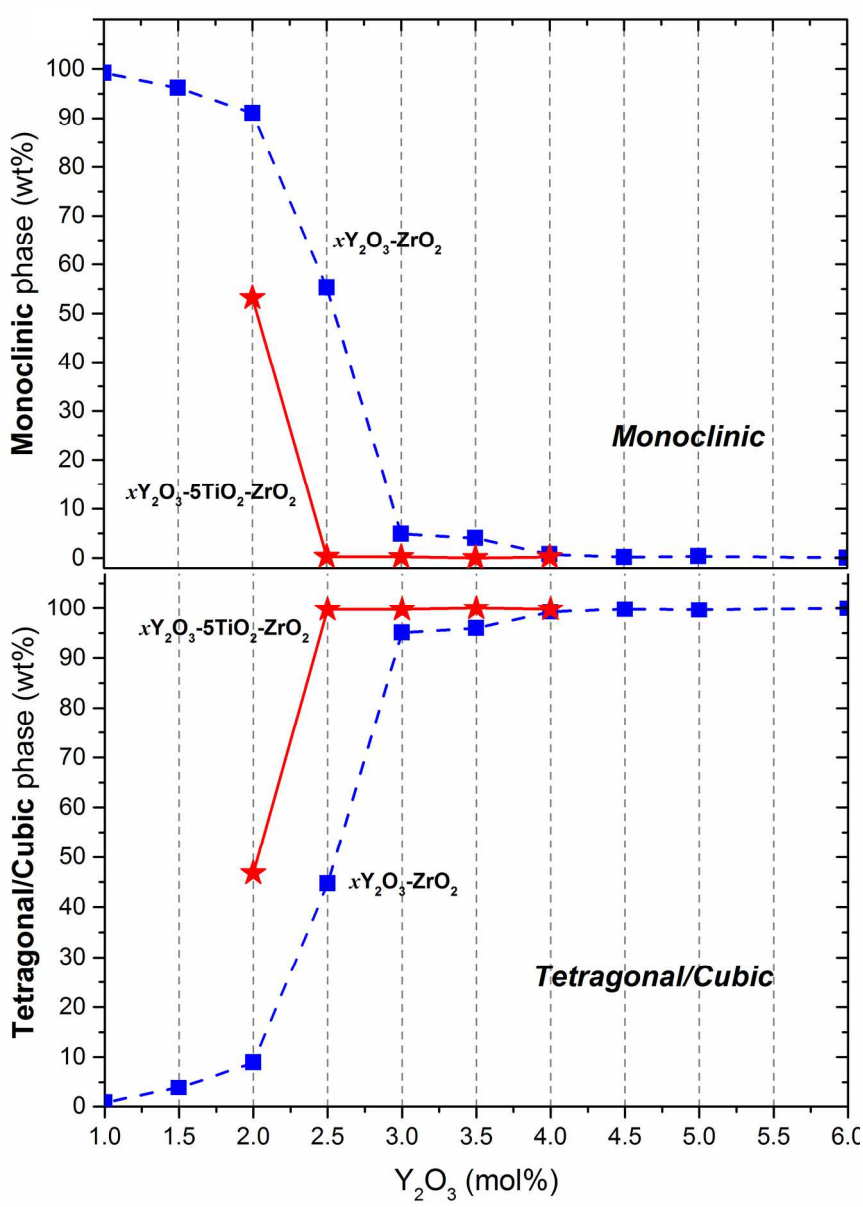

Figure 3: Calculated weight fraction (wt%) of monoclinic phase and the complementary tetragonal/cubic phases (which are not separated in this analysis) in binary Y2O3-ZrO2 and ternary xY2O3-5TiO2-ZrO2 system.
337x471mm (150 x 150 DPI)

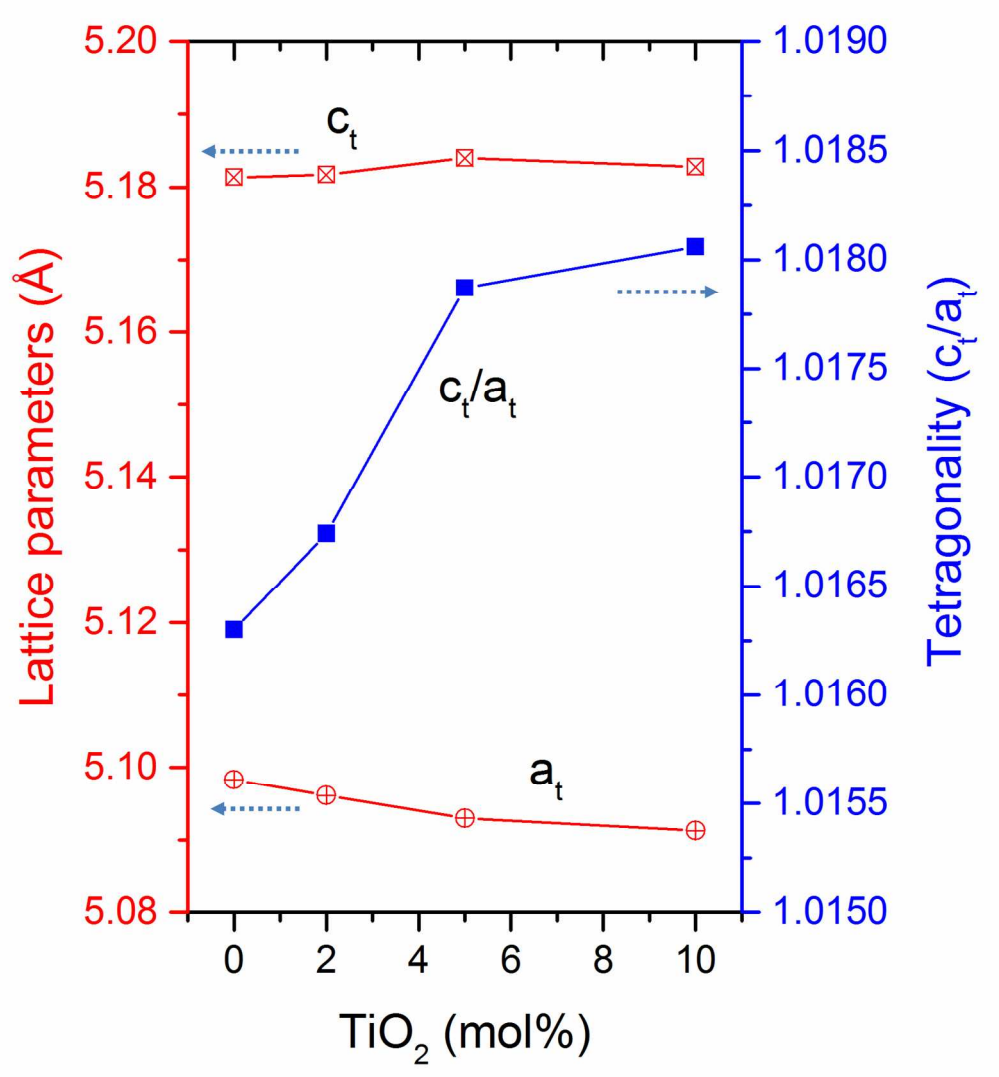

Figure 4: Lattice constants and tetragonality of the tetragonal phase in 3Y2O3-TiO2-ZrO2 as a function of TiO2 concentration.
332x358mm (150 x 150 DPI)

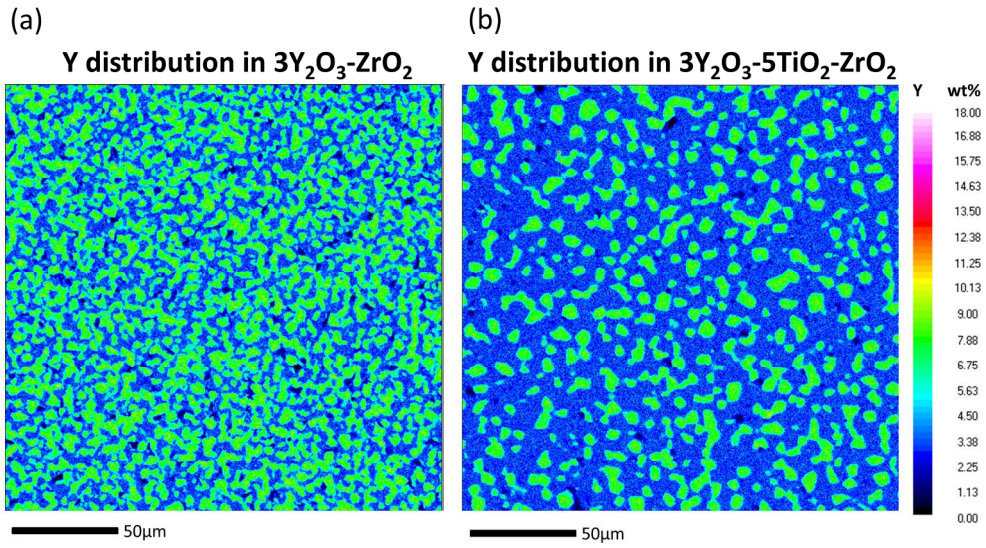

Figure 5: EMPA mapping of yttrium in (a) 3Y2O3-ZrO2 and (b) 3Y2O3-5TiO2-ZrO2 ceramics.
458x258mm (150 x 150 DPI)

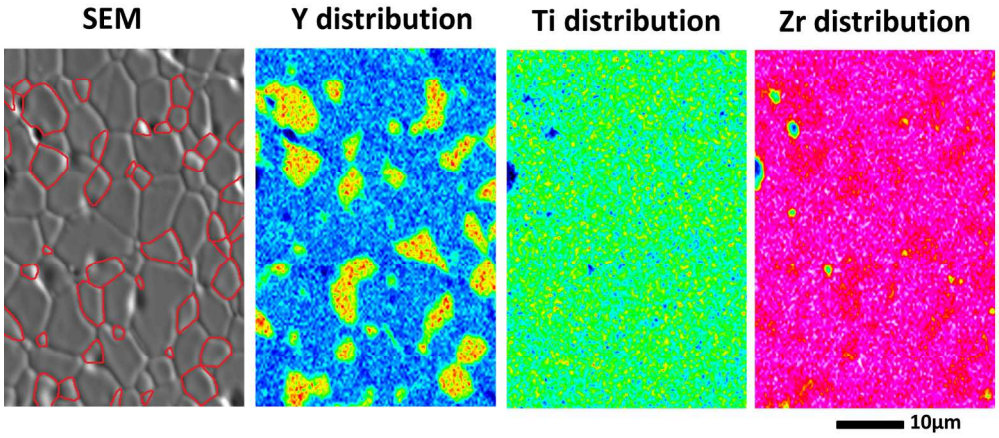

Figure 6: EMPA mapping of 3Y2O3-5TiO2-ZrO2 ceramics, with the SEM images and elemental distributions at the corresponding area. The concentration colour scale is the same as presented in Figure 5.
389x179mm (150 x 150 DPI)

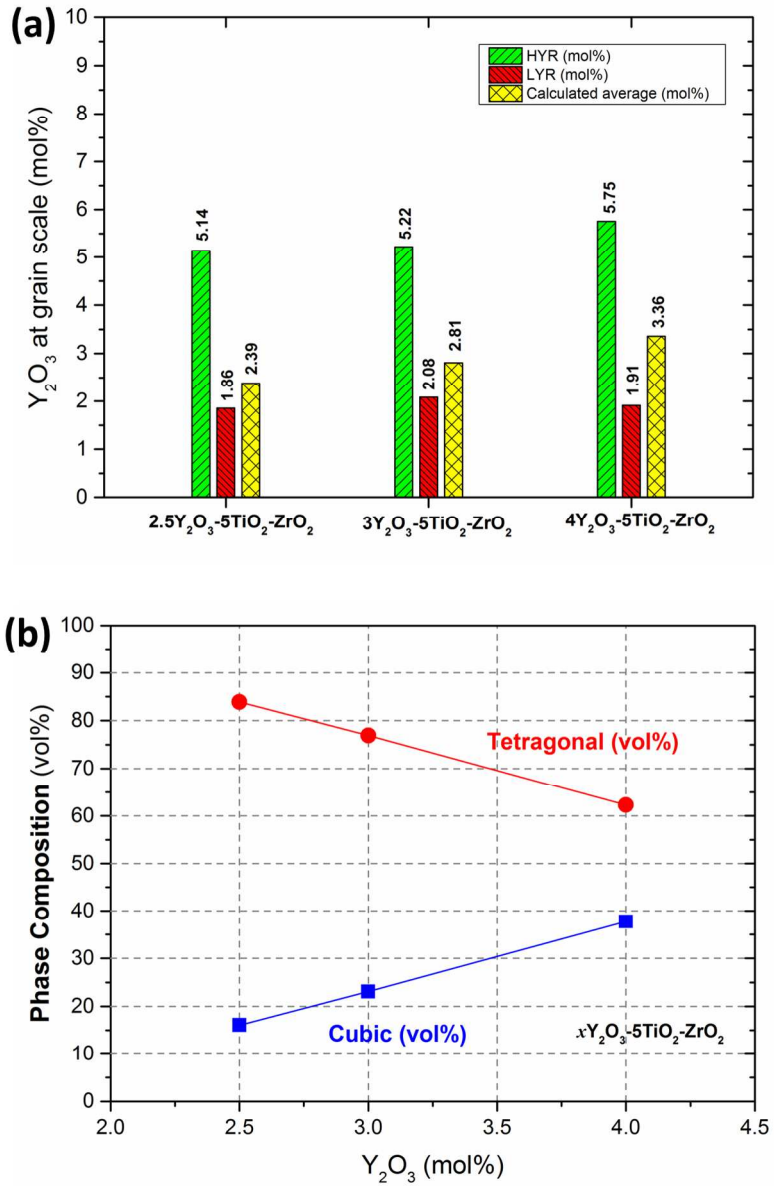

Figure 7: (a) Localized concentration of Y2O3 for high yttrium region (HYR) and low yttrium region (LYR). (b) The phase fraction of tetragonal phase (LYR) and cubic phase (HYR) in xY2O3-5TiO2-ZrO2 system. 241x362mm (150 x 150 DPI)

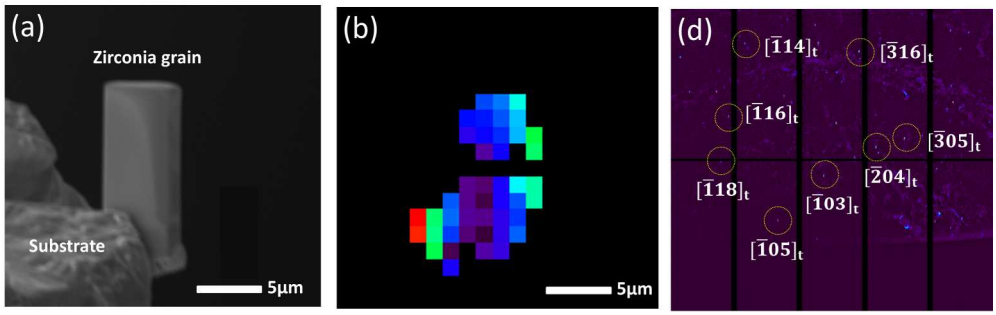

Figure 8: (a) SEM image of the grain cut from the LYR region of 3Y2O3-5TiO2-ZrO2 ceramics, (b) the orientation map of the grain, (c) the corresponding Laue diffraction pattern.
437x138mm (150 x 150 DPI)

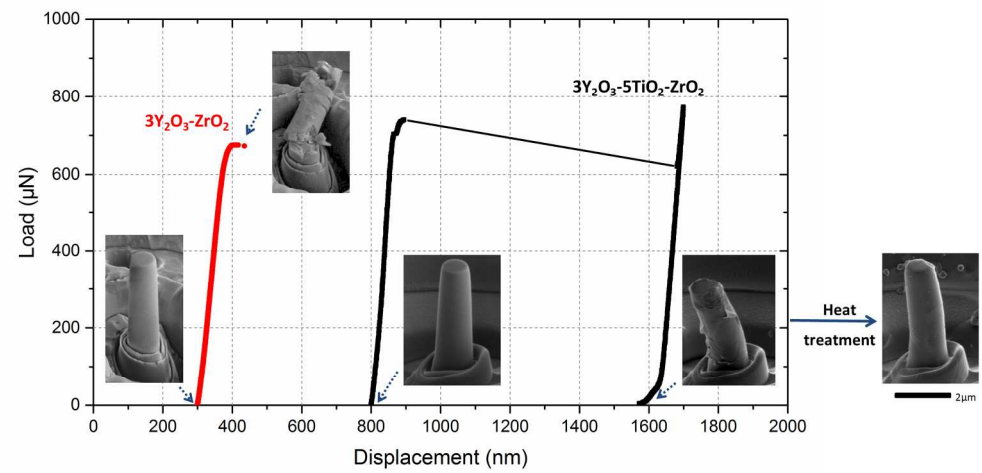

Figure 9: Load-displacement curves of 3Y2O3-ZrO2 and 3Y2O3-5TiO2-ZrO2 pillars, and the corresponding SEM images before and after micro-compression, and after heating at 500oC.
381x180mm (150 x 150 DPI)